PHYSICAL REVIEW C **68**, 041001(R) (2003)

Accurate charge-dependent nucleon-nucleon potential at fourth order of chiral perturbation theory

D. R. Entem[1,2,*] and R. Machleidt[1,†]
[1]*Department of Physics, University of Idaho, Moscow, Idaho 83844, USA*
[2]*Nuclear Physics Group, University of Salamanca, E-37008 Salamanca, Spain*
(Received 8 April 2003; published 31 October 2003)

We present the first nucleon-nucleon potential at next-to-next-to-next-to-leading order (fourth order) of chiral perturbation theory. Charge dependence is included up to next-to-leading order of the isospin-violation scheme. The accuracy for the reproduction of the nucleon-nucleon (*NN*) data below 290-MeV lab energy is comparable to the one of phenomenological high-precision potentials. Since *NN* potentials of order three and less are known to be deficient in quantitative terms, the present work shows that the fourth order is necessary and sufficient for a *NN* potential reliable up to 290 MeV. The new potential provides a promising starting point for exact few-body calculations and microscopic nuclear structure theory (including chiral many-body forces derived on the same footing).

DOI: 10.1103/PhysRevC.68.041001 PACS number(s): 21.30.−x, 13.75.Cs, 12.39.Fe

The theory of nuclear forces has a long history. Based upon the Yukawa idea [1], first field-theoretic attempts [2,3] to derive the nucleon-nucleon (*NN*) interaction focused on pion-exchange, resulting in the *NN* potentials by Gartenhaus [4] and by Signell *et al.* [5]. However, even qualitatively, these potentials barely agreed with empirical information on the nuclear force. So, these "pion theories" of the 1950s are generally judged as failures—for reasons we understand today: pion dynamics is constrained by chiral symmetry, a crucial point that was unknown in the 1950s.

Historically, the experimental discovery of heavy mesons [6] in the early 1960s saved the situation. The one-boson-exchange model [7,8] emerged which is still the most economical and quantitative phenomenology for describing the nuclear force [9,10]. The weak point of this model, however, is the scalar-isoscalar "sigma" or "epsilon" boson, for which the empirical evidence remains controversial. Since this boson is associated with the correlated (or resonant) exchange of two pions, a vast theoretical effort that occupied more than a decade was launched to derive the 2π-exchange contribution of the nuclear force, which creates the intermediate range attraction. For this, dispersion theory as well as field theory were invoked producing the Paris [11,12] and the Bonn [8,13] potentials.

The nuclear force problem appeared to be solved; however, with the discovery of quantum chromodynamics (QCD), all "meson theories" had to be relegated to models and the attempts to derive the nuclear force started all over again.

The problem with a derivation from QCD is that this theory is nonperturbative in the low-energy regime characteristic of nuclear physics, which makes direct solutions impossible. Therefore, during the first round of new attempts, QCD-inspired quark models [14] became popular. These models were able to reproduce qualitatively some of the gross features of the nuclear force. However, on a critical note, it has been pointed out that these quark-based approaches were nothing but another set of models and, thus, did not represent any fundamental progress. Equally well, one may then stay with the simpler and much more quantitative meson models.

A major breakthrough occurred when the concept of an effective field theory was introduced and applied to low-energy QCD. As outlined by Weinberg in a seminal paper [15], one has to write down the most general Lagrangian consistent with the assumed symmetry principles, particularly the (broken) chiral symmetry of QCD. At low energy, the effective degrees of freedom are pions and nucleons rather than quarks and gluons; heavy mesons and nucleon resonances are "integrated out." So, in a certain sense we are back to the 1950s, except that we are smarter by 40 years of experience: broken chiral symmetry is a crucial constraint that generates and controls the dynamics and establishes a clear connection with the underlying theory, QCD.

The chiral effective Lagrangian is given by an infinite series of terms with increasing number of derivatives and/or nucleon fields, with the dependence of each term on the pion field prescribed by the rules of broken chiral symmetry [16]. Applying this Lagrangian to *NN* scattering generates an unlimited number of Feynman diagrams, which may suggest again an untractable problem. However, Weinberg showed [16] that a systematic expansion of the nuclear potential exists in terms of $(Q/\Lambda_\chi)^\nu$, where Q denotes a momentum or pion mass, $\Lambda_\chi \approx 1$ GeV is the chiral symmetry breaking scale, and $\nu \geqslant 0$. For a given order ν, the number of contributing terms is finite and calculable; these terms are uniquely defined and the prediction at each order is model independent. By going to higher orders, the amplitude can be calculated to any desired accuracy. The scheme just outlined has become known as chiral perturbation theory (χPT).

Following the first initiative by Weinberg [16], pioneering work was performed by Ordóñez, Ray, and van Kolck [17,18] who constructed a *NN* potential in coordinate space

*Electronic address: dentem@uidaho.edu, entem@usal.es
†Electronic address: machleid@uidaho.edu

TABLE I. Low-energy constants applied in the N^{3}LO *NN* potential (column "*NN*"). The c_i belong to the dimension-two πN Lagrangian and are in units of GeV^{-1}, while the $\bar{d}_i$ are associated with the dimension-three Lagrangian and are in units of GeV^{-2}. The column "πN" shows values determined from πN data.

	NN	πN
c_1	−0.81	-0.81 ± 0.15[a]
c_2	2.80	3.28 ± 0.23[b]
c_3	−3.20	-4.69 ± 1.34[a]
c_4	5.40	3.40 ± 0.04[a]
$\bar{d}_1+\bar{d}_2$	3.06	3.06 ± 0.21[b]
$\bar{d}_3$	−3.27	-3.27 ± 0.73[b]
$\bar{d}_5$	0.45	0.45 ± 0.42[b]
$\bar{d}_{14}-\bar{d}_{15}$	−5.65	-5.65 ± 0.41[b]

[a]Table 1, Fit 1 of Ref. [35].
[b]Table 2, Fit 1 of Ref. [36].

based upon χPT at next-to-next-to-leading order (NNLO; $\nu=3$). The results were encouraging and many researchers [19] became attracted to the new field. Kaiser *et al.* [20] presented the first model-independent prediction for the *NN* amplitudes of peripheral partial waves at NNLO. Epelbaum *et al.* [21] developed the first momentum-space *NN* potential at NNLO.

In the 1990s, unrelated, parallel research based upon boson-exchange and phenomenological potentials showed that, for conclusive few-body calculations and meaningful microscopic nuclear structure predictions, the input *NN* potential must be of the highest precision; i.e., it must reproduce the *NN* data below about 300-MeV lab energy with a χ^2/datum$\approx$1. The family of high-precision *NN* potentials [9,10,22,23] was developed which fulfills this requirement. Due to the outstanding accuracy of these *NN* potentials, it was possible to pin down cases of few-body scattering and of nuclear structure that clearly require three-nucleon forces (3NF) for their microscopic explanation. Famous examples are the A_y puzzle of *N-d* scattering [24] and the ground state of ^{10}B [25].

One important advantage of χPT is that it makes specific predictions for many-body forces. For a given order of χPT, both 2N and 3N forces are generated on the same footing. At next-to-leading order (NLO), all 3NF cancel [16,26]; however, at NNLO and higher orders, well-defined, nonvanishing 3NF terms occur [26,27]. Since 3NF show up first at NNLO, they are generally small. Therefore, it is only possible to demonstrate their relevance when the 2NF is of high precision (and, of course, of the same order).

NN potentials based upon χPT at NNLO are poor in quantitative terms; they reproduce the *NN* data below 290-MeV lab energy with a χ^2/datum of more than 20. Clearly, there is a strong need for more precision, implying that going to higher order is necessary.

It is the purpose of this note to present the first *NN* potential that is based consistently on χPT at next-to-next-to-next-to-leading order (N^{3}LO; fourth order). We will show that, at this order, the accuracy is comparable to the one of the high-precision phenomenological potentials. Thus, the *NN* potential at N^{3}LO is the first to meet the requirements for a reli-

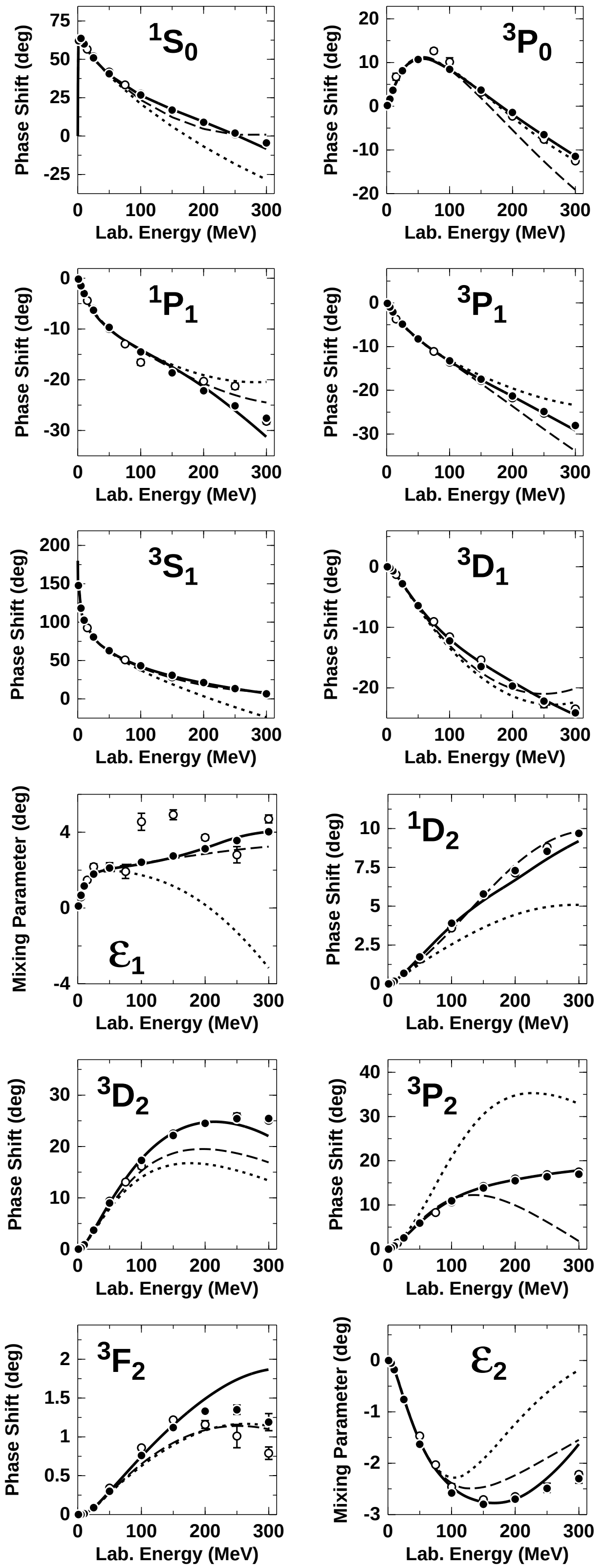

FIG. 1. *np* phase parameters below 300-MeV lab energy for partial waves with $J\leqslant2$. The solid line is the result at N^{3}LO. The dotted and dashed lines are the phase shifts at NLO and NNLO, respectively, as obtained by Epelbaum *et al.* [37]. The solid dots show the Nijmegen multienergy *np* phase shift analysis [38], and the open circles are the VPI single-energy *np* analysis SM99 [39].

TABLE II. χ^2/datum for the reproduction of the 1999 *np* database [40] below 290 MeV by various *np* potentials.

Bin (MeV)	No. of data	N^{3}LO[a]	NNLO[b]	NLO[b]	AV18[c]
0–100	1058	1.06	1.71	5.20	0.95
100–190	501	1.08	12.9	49.3	1.10
190–290	843	1.15	19.2	68.3	1.11
0–290	2402	1.10	10.1	36.2	1.04

[a]This work.
[b]Reference [37].
[c]Reference [22].

able input potential for exact few-body and microscopic nuclear structure calculations (including chiral 3NF consistent with the chiral 2NF).

In χPT, the *NN* amplitude is uniquely determined by two classes of contributions: contact terms and pion-exchange diagrams. At N^{3}LO, there are two contacts of order $Q^0[O(Q^0)]$, seven of $O(Q^2)$, and 15 of $O(Q^4)$, resulting in a total of 24 contact terms, which generate 24 parameters that are crucial for the fit of the partial waves with orbital angular momentum $L \leqslant 2$ [28].

Now, turning to the pion contributions: At leading order [LO,$O(Q^0)$, ν=0], there is only the well-known static one-pion exchange (OPE). Two-pion exchange (TPE) starts at NLO (ν=2), and there are further TPE contributions in any higher order. While TPE at NNLO was known for a while [17,20,21], TPE at N^{3}LO has been calculated only recently by Kaiser [29]. All 2π exchange contributions up to N^{3}LO are summarized in a pedagogical and systematic fashion in Ref. [30] where the model-independent results for *NN* scattering in peripheral partial waves are also shown. We use the analytic expressions published in Ref. [30], except for one small modification. Since our iterated OPE is not identical to Eq. (24) of Ref. [20], we have changed the relativistic $1/M_N$ corrections contained in Eqs. (21)–(24) of Ref. [30] such that they match our iterated OPE. The details will be published elsewhere [31].

Finally, there is also three-pion exchange, which shows up for the first time at N^{3}LO (two loops). In Ref. [32], it was demonstrated that the 3π contributions at this order are negligible, which is why we leave them out.

For an accurate fit of the low-energy *pp* and *np* data, charge dependence is important. We include charge dependence up to next-to-leading order of the isospin-violation scheme (NLØ, in the notation of Ref. [33]). Thus, we include the pion mass difference in OPE and the Coulomb potential in *pp* scattering, which takes care of the LØ contributions. At order NLØ we have pion mass difference in the NLO part of TPE, $\pi\gamma$ exchange [34], and two charge-dependent contact interactions of order Q^0 which make possible an accurate fit of the three different $^1S_0$ scattering lengths a_{pp}, a_{nn}, and a_{np}.

TABLE III. χ^2/datum for the reproduction of the 1999 *pp* database [40] below 290 MeV by various *pp* potentials.

Bin (MeV)	No. of data	N^{3}LO[a]	NNLO[b]	NLO[b]	AV18[c]
0–100	795	1.05	6.66	57.8	0.96
100–190	411	1.50	28.3	62.0	1.31
190–290	851	1.93	66.8	111.6	1.82
0–290	2057	1.50	35.4	80.1	1.38

[a]This work.
[b]See footnote [41].
[c]Reference [22].

TABLE IV. Scattering lengths (a) and effective ranges (r) in units of femtometer. (a^C_{pp} and r^C_{pp} refer to the *pp* parameters in the presence of the Coulomb force. a^N and r^N denote parameters determined from the nuclear force only and with all electromagnetic effects omitted.)

	N^{3}LO[a]	Experiment[b]
	$^1S_0$	
a^C_{pp}	−7.8188	−7.8196±0.0026
r^C_{pp}	2.795	2.790±0.014
a^N_{pp}	−17.083	
r^N_{pp}	2.876	
a^N_{nn}	−18.900	−18.9±0.4
r^N_{nn}	2.838	2.75±0.11
a_{np}	−23.732	−23.740±0.020
r_{np}	2.725	2.77±0.05
	$^3S_1$	
a_t	5.417	5.419±0.007
r_t	1.752	1.753±0.008

[a]This work.
[b]See Table XIV of Ref. [10] for references.

Chiral perturbation theory is a low-momentum expansion. It is valid only for momenta $Q \ll \Lambda_\chi \approx 1$ GeV. To enforce this, we multiply all expressions (contacts and irreducible pion exchanges) with a regulator function,

$$\exp\left[-\left(\frac{p}{\Lambda}\right)^{2n}-\left(\frac{p'}{\Lambda}\right)^{2n}\right], \tag{1}$$

where p and p' denote, respectively, the magnitudes of the initial and final nucleon momenta in the center-of-mass frame. We use Λ=0.5 GeV throughout. The exponent $2n$ is chosen to be sufficiently large so that the regulator generates powers which are beyond the order (ν=4) at which our calculation is conducted. Thus, we use $n \geqslant 3$ for LO contributions and $n \geqslant 2$ for NLO and higher order.

The contact terms plus irreducible pion-exchange expressions at N^{3}LO, multiplied by the above regulator, define the *NN* potential at N^{3}LO. This potential is applied in a Lippmann-Schwinger equation to obtain the T matrix from which phase shifts and *NN* observables are calculated. The corresponding homogenous equation determines the properties of the two-nucleon bound state (deuteron).

The peripheral partial waves of *NN* scattering with $L \geqslant 3$ are exclusively determined by OPE and TPE because the N^{3}LO contacts contribute to $L \leqslant 2$ only. OPE and TPE at N^{3}LO depend on the axial-vector coupling constant g_A (we use g_A=1.29), the pion decay constant f_π=92.4 MeV, and eight low-energy constants (LEC) that appear in the dimension-two and dimension-three πN Lagrangians (cf.

TABLE V. Two- and three-nucleon bound-state properties. (Deuteron binding energy B_d; asymptotic S state A_S; asymptotic D/S state η; deuteron radius r_d; quadrupole moment Q; D-state probability P_D; triton binding energy B_t.)

	N^3LO[a]	CD-Bonn [10]	AV18 [22]	Empirical[b]
Deuteron				
B_d(MeV)	2.224575	2.224575	2.224575	2.224575(9)
A_S(fm$^{-1/2}$)	0.8843	0.8846	0.8850	0.8846(9)
η	0.0256	0.0256	0.0250	0.0256(4)
r_d(fm)	1.978[c]	1.970[c]	1.971[c]	1.97535(85)
Q(fm^2)	0.285[d]	0.280[d]	0.280[d]	0.2859(3)
P_D(%)	4.51	4.85	5.76	
Triton				
B_t(MeV)[e]	7.855	8.00	7.62	8.48

[a]This work.
[b]See Table XVIII of Ref. [10] for references.
[c]With meson-exchange currents (MEC) and relativistic corrections (RC) [42].
[d]Including MEC and RC in the amount of 0.010 fm^2.
[e]As obtained in a charge-dependent 34-channel Faddeev calculation applying only 2N forces.

Ref. [30]). In the fitting process, we varied three of them, namely, c_2, c_3, and c_4. We found that the other LEC are not very effective in the NN system and, therefore, we kept them at the values determined from πN (cf. Table I). The most influential constant is c_3, which has to be chosen on the low side (slightly more than one standard deviation below its πN determination) for an optimal fit of the NN data. As compared to a calculation that strictly uses the πN values for c_2 and c_4, our choices for these two LEC lower the $^3F_2$ and $^1F_3$ phase shifts bringing them into closer agreement with the phase shift analysis. The other F waves and the higher partial waves are essentially unaffected by our variations of c_2 and c_4. Overall, the fit of all $J \geqslant 3$ waves (that are not shown in Fig. 1) is excellent.

The most important sets of fit parameters are the ones associated with the 24 contact terms that rule the partial waves with $L \leqslant 2$. In addition, we have two charge-dependent contacts, which bring the number of contact parameters to 26. Since we treated three LEC as semifree, the total number of parameters of the N^3LO potential is 29.

In the optimization procedure, we fit first phase shifts, and then we refine the fit by minimizing the χ^2 obtained from a direct comparison with the data. The phase shifts at N^3LO for np scattering below 300-MeV lab energy are displayed in Fig. 1. The χ^2/datum for the fit of the np data below 290 MeV is shown in Table II, and the corresponding one for pp is given in Table III. Obviously, the χ^2 tables show the quantitative improvement of the NN interaction order by order in a dramatized fashion. Even though there is considerable improvement when going from NLO to NNLO, it is clearly seen that N^3LO is needed to achieve an accuracy comparable to the phenomenological high-precision Argonne V_{18} potential [22].

At this point, a clarifying word is in place concerning how to properly view the aspect of accuracy when working with χPT. One great advantage of χPT is that it allows us to estimate the theoretical uncertainty at any given order. Since χPT is an expansion in Q/Λ_χ, one may estimate the theoretical uncertainty at order ν by calculating $(Q/\Lambda_\chi)^{\nu+1}$, where $Q < \Lambda = 500$ MeV in our case. Thus, for NLO the relative uncertainty is $(Q/\Lambda_\chi)^3 = 13\%$, for NNLO $(Q/\Lambda_\chi)^4 = 6\%$, and for N^3LO $(Q/\Lambda_\chi)^5 = 3\%$. These uncertainties are well reflected in the phase shift plots of Fig. 1. In the case of the χ^2/datum shown in Tables II and III, one needs to keep in mind that the χ^2 is by definition the *square* of the theoretical error over the experimental error. Thus, deviations of the predictions from the experimental values are blown up quadratically. This may explain why the changes in the χ^2, order by order, appear more dramatic. Neutron-proton data carry experimental errors that are typically around 4% which is why at N^3LO a χ^2/datum ≈ 1 can be achieved. Proton-proton data have characteristically smaller experimental errors than np data resulting in larger χ^2.

The low-energy parameters are shown in Table IV and deuteron properties in Table V. The agreement between N^3LO and experiment is excellent throughout. The results for the deuteron radius are remarkable. All NN potentials of the past (Table V includes two representative examples, namely, CD-Bonn[10] and AV18[22]) predict the new empirical value for the deuteron radius (that is obtained by using the isotope-shift method [43]) too small [42]. In contrast, our N^3LO potential predicts the radius slightly too large. Table V also includes the prediction of the triton binding energy as obtained in a charge-dependent 34-channel Faddeev calculation. Note that this calculation includes only 2N forces and that for a complete calculation the 3NF of NNLO and N^3LO need to be included.

In conclusion, we have developed the first NN potential at fourth order of χPT [44]. This potential is as quantitative as some so-called high-precision phenomenological potentials. Due to its basis in χPT, the many-body forces associated with this two-body force are well defined [26,27]. Thus, we have a promising starting point for exact few-body calculations and microscopic nuclear structure theory.

This work was supported by the U.S. National Science Foundation under Grant No. PHY-0099444 and by three Spanish foundations: the Ministerio de Ciencia y Tecnología under Contract No. BFM2001-3563, the Junta de Castilla y León under Contract No. SA-109/01, and the Ramón Areces Foundation.

[1] H. Yukawa, Proc. Phys. Math. Soc. Jpn. **17**, 48 (1935).
[2] M. Taketani *et al.*, Prog. Theor. Phys. **7**, 45 (1952).
[3] K. A. Brueckner *et al.*, Phys. Rev. **90**, 699 (1953); K. A. Brueckner *et al.*, *ibid.* **92**, 1023 (1953).
[4] S. Gartenhaus, Phys. Rev. **100**, 900 (1955).
[5] P. Signell *et al.*, Phys. Rev. **109**, 1229 (1958).
[6] A. R. Erwin *et al.*, Phys. Rev. Lett. **6**, 628 (1961); B. C. Maglić *et al.*, *ibid.* **7**, 178 (1961).
[7] R. A. Bryan and B. L. Scott, Phys. Rev. **177**, 1435 (1969); M. M. Nagels *et al.*, Phys. Rev. D **17**, 768 (1978).
[8] R. Machleidt, Adv. Nucl. Phys. **19**, 189 (1989).
[9] V. G. J. Stoks *et al.*, Phys. Rev. C **49**, 2950 (1994).
[10] R. Machleidt, Phys. Rev. C **63**, 024001 (2001).
[11] R. Vinh Mau, in *Mesons in Nuclei*, edited by M. Rho and D. H. Wilkinson (North-Holland, Amsterdam, 1979), Vol. I, p. 151.
[12] M. Lacombe *et al.*, Phys. Rev. C **21**, 861 (1980).
[13] R. Machleidt *et al.*, Phys. Rep. **149**, 1 (1987).
[14] F. Myhrer *et al.*, Rev. Mod. Phys. **60**, 629 (1988).
[15] S. Weinberg, Physica A **96**, 327 (1979).
[16] S. Weinberg, Phys. Lett. B **251**, 288 (1990); Nucl. Phys. **B363**, 3 (1991).
[17] C. Ordóñez, L. Ray, and U. van Kolck, Phys. Rev. Lett. **72**, 1982 (1994); C. Ordóñez, L. Ray, and U. van Kolck, Phys. Rev. C **53**, 2086 (1996).
[18] U. van Kolck, Prog. Part. Nucl. Phys. **43**, 337 (1999).
[19] L. S. Celenza *et al.*, Phys. Rev. C **46**, 2213 (1992); C. A. da Rocha *et al.*, *ibid.* **49**, 1818 (1994); D. B. Kaplan *et al.*, Nucl. Phys. **B478**, 629 (1996).
[20] N. Kaiser *et al.*, Nucl. Phys. **A625**, 758 (1997).
[21] E. Epelbaum *et al.*, Nucl. Phys. **A637**, 107 (1998); E. Epelbaum *et al.*, *ibid.* **A671**, 295 (2000).
[22] R. B. Wiringa *et al.*, Phys. Rev. C **51**, 38 (1995).
[23] R. Machleidt *et al.*, Phys. Rev. C **53**, 1483 (1996).
[24] W. Glöckle *et al.*, Phys. Rep. **274**, 107 (1996).
[25] E. Caurier *et al.*, Phys. Rev. C **66**, 024314 (2002).
[26] U. van Kolck, Phys. Rev. C **49**, 2932 (1994).
[27] E. Epelbaum *et al.*, Phys. Rev. C **66**, 064001 (2002).
[28] The 24 contacts of N^3LO were included for the first time in an earlier chiral *NN* potential constructed by the authors [D. R. Entem and R. Machleidt, Phys. Lett. B **524**, 93 (2002)] where the outstanding importance of the $O(Q^4)$ contacts for a quantitative reproduction of the *NN D* waves was demonstrated. However, this earlier potential included TPE only up to NNLO.
[29] N. Kaiser, Phys. Rev. C **64**, 057001 (2001); **65**, 017001 (2002).
[30] D. R. Entem and R. Machleidt, Phys. Rev. C **66**, 014002 (2002).
[31] D. R. Entem and R. Machleidt (unpublished).
[32] N. Kaiser, Phys. Rev. C **61**, 014003 (1999); **62**, 024001 (2000).
[33] M. Walzl *et al.*, Nucl. Phys. **A693**, 663 (2001).
[34] U. van Kolck *et al.*, Phys. Rev. Lett. **80**, 4386 (1998).
[35] P. Büttiker *et al.*, Nucl. Phys. **A668**, 97 (2000).
[36] N. Fettes *et al.*, Nucl. Phys. **A640**, 199 (1998).
[37] E. Epelbaum *et al.*, Eur. Phys. J. A **15**, 543 (2002).
[38] V. G. J. Stoks *et al.*, Phys. Rev. C **48**, 792 (1993).
[39] SAID, solution SM99 (1999).
[40] The 1999 *NN* data base is defined in Ref. [10].
[41] Since Ref. [37] provides only the *np* versions of the NLO and NNLO potentials, we have constructed the *pp* versions by incorporating charge dependence and minimizing the *pp* χ^2.
[42] J. L. Friar *et al.*, Phys. Rev. A **56**, 4579 (1997).
[43] A. Huber *et al.*, Phys. Rev. Lett. **80**, 468 (1998).
[44] A user-friendly computer code for the N^3LOpotential is available from the authors upon request.